

Spin-glass attractor on tridimensional hierarchical lattices in the presence of an external magnetic field

Octavio R. Salmon^{*} and Fernando D. Nobre[†]

Centro Brasileiro de Pesquisas Físicas and National Institute of Science and Technology for Complex Systems, Rua Xavier Sigaud 150, 22290-180 Rio de Janeiro, RJ, Brazil

(Received 25 October 2008; revised manuscript received 11 February 2009; published 20 May 2009)

A nearest-neighbor-interaction Ising spin glass, in the presence of an external magnetic field, is studied on different hierarchical lattices that approach the cubic lattice. The magnetic field is considered as uniform or random (following either a bimodal or a Gaussian probability distribution). In all cases, a spin-glass attractor is found, in the plane magnetic field versus temperature, associated with a low-temperature phase. The physical consequences of this attractor are discussed, in view of the present scenario of the spin-glass problem.

DOI: [10.1103/PhysRevE.79.051122](https://doi.org/10.1103/PhysRevE.79.051122)

PACS number(s): 05.50.+q, 75.10.Nr, 75.50.Lk, 64.60.-i

I. INTRODUCTION

Short-range-interaction spin-glass (SG) models [1–4] have raised a lot of controversies in the last decades. From the theoretical point of view, the case of Ising spins represents the most convenient to be investigated, in such a way that a large effort has been dedicated to the understanding of the Ising SG model. The majority of works concentrated on three-dimensional Ising SG models, for which, besides its physical realizations, it is generally accepted nowadays that a SG phase occurs at finite temperatures [5–13].

Hierarchical lattices have been a very useful tool for the study of SG models [5,8,14–26], essentially due to the possibility of carrying out exact calculations, or performing relatively low-time-consuming numerical computations. Apart from a few exceptions [17,23,25,26], most of the hierarchical lattices considered so far belong to the Migdal-Kadanoff (MK) family. Taking into account the significant reduction of efforts in the investigation of these models, some of the results obtained are quite impressive: (i) the lower critical dimension, below which the SG phase transition occurs at zero temperature, which was the object of a lot of controversy about 3 decades ago, was correctly estimated within a MK renormalization-group (RG) approach [5], almost 1 decade before the consensus that this quantity should be greater than 2, but smaller than 3, through different numerical approaches, such as numerical simulations [6,7,9] and zero-temperature domain-wall arguments [8]. (ii) The critical-temperature estimates of Ref. [5] for an Ising SG on a MK hierarchical lattice of fractal dimension $D=3$, with symmetric distributions, are $(k_B T_c / J) = 1.05 \pm 0.02$ ($\pm J$ distribution) and $(k_B T_c / J) = 0.88 \pm 0.02$ (Gaussian distribution of width J). The most recent Monte Carlo simulations on a cubic lattice [12] yield $(k_B T_c / J) = 1.120 \pm 0.004$ in the first case, whereas for the latter, $(k_B T_c / J) = 0.951 \pm 0.009$, leading to relative discrepancies of about 4% when compared to the results of Ref. [5], taking into account the error bars. (iii) A zero-temperature analysis of a Gaussian Ising SG, on a special hierarchical lattice with fractal dimension $D=2$ [17], yielded

an estimate for the stiffness exponent y ($y = -1/\nu$, where ν is the exponent associated with the divergence of the correlation length at zero temperature) in agreement with those obtained from other, more time-consuming, numerical approaches. (iv) The same hierarchical lattice of Ref. [17], mentioned above, produced a precise ferromagnetic-paramagnetic critical frontier for the $\pm J$ Ising SG model [25].

A major question in the SG problem nowadays concerns the applicability of some results from the mean-field solution for short-range-interaction systems. In particular, whether the SG phase is properly described by an infinite number of order parameters (i.e., an order-parameter function [27]), manifesting the property of replica-symmetry breaking (RSB) [10]; moreover, if an Ising SG, in the presence of an external magnetic field, exhibits the Almeida-Thouless (AT) line [28], which separates a low-temperature region characterized by RSB, from a high-temperature one, described in terms of a single order parameter, along which the replica-symmetric solution holds. Numerical simulations for nearest-neighbor-interaction Ising SGs are always hard to perform since equilibration becomes difficult for large system sizes and low temperatures. However, in spite of the small lattice sizes considered, there are evidences from Monte Carlo simulations that a critical line in the presence of a field exists in $d=4$ [29], but not in $d=3$ [11,13]. Furthermore, a zero-temperature analysis of the energy landscape in the case $d=3$ is compatible with a transition from the SG to the paramagnetic phase for a finite critical field, although the possibility of a critical field equal to zero was not excluded [30]. However, it is possible to have a critical frontier separating the SG and paramagnetic phases, for low-dimensional short-range-interaction Ising SGs in the presence of a magnetic field, which is not an AT-type line. In order to ensure that this critical line represents a true AT line, one should also verify evidences of RSB below such a frontier. This possibility would correspond to an “intermediate” scenario [30] between the mean-field RSB solution and the much simpler droplet picture [1–3]. In this case, one would expect that RSB effects should appear below this line, at some finite dimension d , contrary to claims of the droplet model, according to which the AT line should occur only in the limit of infinite dimensions.

^{*}octavior@cbpf.br

[†]Corresponding author; fdnobre@cbpf.br

One of the advantages for the study of SGs on hierarchical lattices is that one does not go through equilibration difficulties. In view of this, the $D=3$ MK hierarchical lattice has been used also for an investigation of RSB in the low-temperature phase on an Ising SG without a magnetic field [18,21,22,24]. For temperatures in the range $0.7 T_c < T < T_c$, a picture showing characteristics of RSB was observed, although for lower temperatures the results agree with the simpler, replica-symmetric scenario.

To our knowledge, short-range-interaction SGs in the presence of an external magnetic field have never been investigated on hierarchical lattices. In the present work, we study an Ising SG model, in the presence of different types of external magnetic fields, on three hierarchical lattices (two of them with a fractal dimension $D=3$ and another one characterized by $D \approx 3.58$). In the next section we define the model, the hierarchical lattices, and the numerical procedure. In Sec. III we present and discuss our results.

II. MODEL AND NUMERICAL PROCEDURE

Herein, we study an Ising SG in the presence of an external magnetic field

$$\mathcal{H} = - \sum_{\langle ij \rangle} J_{ij} S_i S_j - \sum_i h_i S_i \quad (S_i = \pm 1), \quad (1)$$

where $\{J_{ij}\}$ denote random couplings between two spins located at nearest-neighboring sites i and j of a given hierarchical lattice, following a symmetric Gaussian probability distribution,

$$P(J_{ij}) = \frac{1}{\sqrt{2\pi J^2}} \exp\left(-\frac{J_{ij}^2}{2J^2}\right). \quad (2)$$

For the magnetic fields we consider three different cases, namely,

$$P(h_i) = \delta(h_i - H_0) \quad (\text{uniform field}), \quad (3)$$

$$P(h_i) = \frac{1}{2} \delta(h_i - H_0) + \frac{1}{2} \delta(h_i + H_0) \quad (\text{symmetric bimodal distribution}), \quad (4)$$

$$P(h_i) = \frac{1}{\sqrt{2\pi\sigma^2}} \exp\left[-\frac{(h_i - H_0)^2}{2\sigma^2}\right] \quad (\text{Gaussian distribution}). \quad (5)$$

The Hamiltonian of Eq. (1) will be investigated on three different hierarchical lattices that approach the cubic lattice. These lattices are generated by starting the process from the 0th level of the lattice-generation hierarchy, with a single bond joining the external sites (denoted by μ and ν). Then, in each iteration step one replaces a single bond by a unit cell, such as the ones shown in Fig. 1, in such a way that in its first hierarchy, each lattice is represented by a unit cell; the hierarchical lattice is constructed up to a given \mathcal{N} th hierarchy ($\mathcal{N} \gg 1$). The cells in Figs. 1(a) and 1(b) are considered as dual to one another and their results for critical temperatures

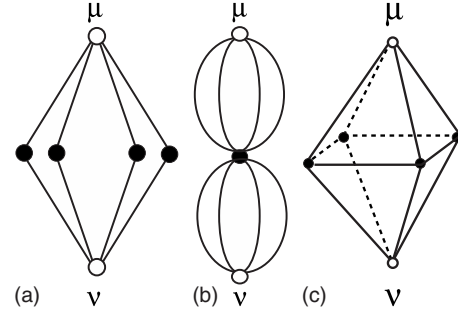


FIG. 1. Basic cells of three hierarchical lattices that approach the cubic lattice. (a) The MK cell of fractal dimension $D=3$ (usually called of diamond cell). (b) The dual of the diamond cell (fractal dimension $D=3$). (c) The tridimensional Wheatstone-Bridge cell (fractal dimension $D \approx 3.58$). Empty circles represent the external sites, whereas black circles are sites to be decimated in the renormalization process.

usually represent the lower and upper limits, respectively, with respect to the correct value of the cubic lattice [31]. The cell of Fig. 1(c) is a three-dimensional Wheatstone Bridge cell and, to our knowledge, it has never been used in the study of random magnetic models.

The RG procedure works in the inverse way of the lattice generation, i.e., through a decimation of the internal sites of a given cell, leading to renormalized quantities associated with the external sites. Defining the dimensionless couplings and fields, $K_{ij} = \beta J_{ij}$ and $H_i = \beta h_i$ [$\beta = 1/(k_B T)$], the corresponding RG equations may be written in the general form [see Ref. [32] for the explicit form of these equations for the MK cell of Fig. 1(a)]

$$K'_{\mu\nu} = \frac{1}{4} \log\left(\frac{Z_{--}Z_{++}}{Z_{+-}Z_{-+}}\right), \quad (6)$$

$$H'_\mu = \frac{1}{4} \log\left(\frac{Z_{++}Z_{+-}}{Z_{--}Z_{-+}}\right), \quad (7)$$

$$H'_\nu = \frac{1}{4} \log\left(\frac{Z_{++}Z_{-+}}{Z_{--}Z_{+-}}\right), \quad (8)$$

where $Z_{S_\mu S_\nu}$ represent partition functions of a given cell with the external spins kept fixed ($S_\mu, S_\nu = \pm 1$),

$$Z_{S_\mu S_\nu} = \text{Tr}_{\{S_i (i \neq \mu, \nu)\}} [\exp(-\beta \mathcal{H})]. \quad (9)$$

It should be noticed that the Hamiltonian associated with any of the cells of Fig. 1 may be split into $\mathcal{H} = \mathcal{H}' + H_\mu S_\mu + H_\nu S_\nu$, where \mathcal{H}' represents the Hamiltonian of the cell with $H_\mu = H_\nu = 0$. Therefore, the partition function $Z_{S_\mu S_\nu}$ may be rewritten as

$$Z_{S_\mu S_\nu} = \exp(H_\mu S_\mu + H_\nu S_\nu) \mathcal{Z}_{S_\mu S_\nu}, \quad (10)$$

where

$$\mathcal{Z}_{S_\mu S_\nu} = \text{Tr}_{\{S_i (i \neq \mu, \nu)\}} [\exp(-\beta \mathcal{H}')] \quad (11)$$

represents the partition function of a given cell without considering the contributions of the fields on its external sites.

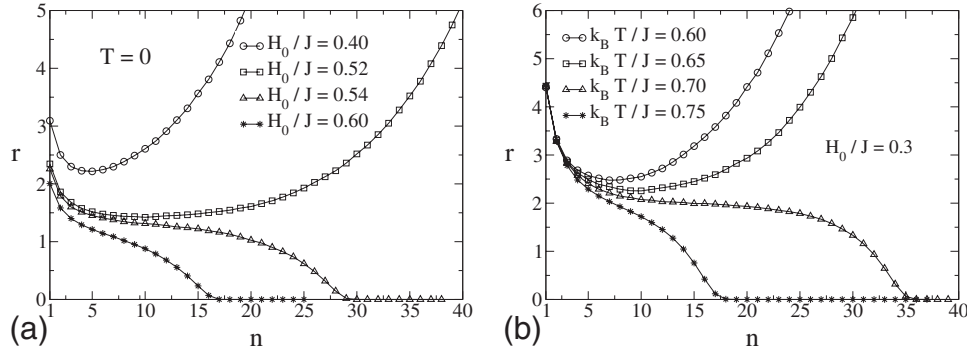


FIG. 2. Evolution of the ratio r with the RG steps n , for an Ising SG on the hierarchical lattice defined by the unit cell of Fig. 1(a), in the presence of an initial uniform field H_0 . (a) Typical values of H_0/J at zero temperature; the critical field is in the range $0.52 < (H_{0c}/J) < 0.54$. (b) Typical temperatures for $(H_0/J)=0.3$; the critical temperature is in the range $0.65 < (k_B T_c/J) < 0.70$.

Accordingly, Eqs. (6)–(8) take the following form

$$K'_{\mu\nu} = \frac{1}{4} \log \left(\frac{\mathcal{Z}_{--}\mathcal{Z}_{++}}{\mathcal{Z}_{+-}\mathcal{Z}_{-+}} \right), \quad (12)$$

$$H'_\mu = H_\mu + \frac{1}{4} \log \left(\frac{\mathcal{Z}_{++}\mathcal{Z}_{+-}}{\mathcal{Z}_{--}\mathcal{Z}_{-+}} \right), \quad (13)$$

$$H'_\nu = H_\nu + \frac{1}{4} \log \left(\frac{\mathcal{Z}_{++}\mathcal{Z}_{-+}}{\mathcal{Z}_{--}\mathcal{Z}_{+-}} \right). \quad (14)$$

Thus, we clearly see through Eqs. (13) and (14) that after the RG transformation, the field on each remaining site depends on the previous field on this site plus a contribution due to the decimation of the inner spins in the cell.

If at the beginning of the RG procedure (\mathcal{N} th hierarchy), one uses the probability distribution of Eq. (2) for the couplings and one of the probability distributions of Eqs. (3)–(5) for the fields, one has at this level the average values $\langle K_{ij} \rangle = 0$ and $\langle H_i \rangle = H_0$ (uniform field and Gaussian distribution) or $\langle H_i \rangle = 0$ (symmetric bimodal distribution). An important quantity to be used herein is the ratio of associated widths,

$$r = \frac{\sigma_K}{\sigma_H}; \quad \sigma_K = \langle (K_{ij} - \langle K_{ij} \rangle)^2 \rangle^{1/2}; \quad \sigma_H = \langle (H_i - \langle H_i \rangle)^2 \rangle^{1/2}, \quad (15)$$

which, at the \mathcal{N} th level, is infinite for a uniform field (since $\sigma_H = 0$ in this case), whereas $r = J/H_0$ (bimodal distribution) and $r = J/\sigma$ (Gaussian distribution for the fields). However, as the renormalization procedure goes on (in fact, right after the first RG transformation), the system of coupled equations that define the renormalization [Eqs. (6)–(8)] introduces correlations between the couplings and fields, and as a result of this, one has a joint probability distribution, $P(K_{ij}, H_i, H_j)$, to be followed.

We have used the method proposed in Ref. [33] to follow this distribution numerically. This technique consists in generating a pool of M triplets $\{K_{ij}, H_i, H_j\}$, initially chosen by generating random numbers according to the above distribution for the couplings, and one of the probability distributions for the fields. An iteration consists in M operations, where in each of them one picks randomly triplets from the

pool (each chosen triplet is assigned to a bond in one of the cells of Fig. 1) in order to generate the effective quantities of Eqs. (6)–(8) that will define a triplet of the renormalized pool. At zero temperature Eqs. (6)–(8) become much simpler [see, e.g., Ref. [32] for the explicit form of these equations for the MK cell of Fig. 1(a)] and we have used these simplified forms to determine the zero-temperature critical points. It is important to notice that in this procedure there may occur superpositions of random fields in given sites of the unit cells; whenever this happens, we consider an arithmetic average of the superposed random fields. After each iteration, one calculates the lowest moments associated with the couplings and fields and, in particular, the ratio r defined in Eq. (15). Below, we present and discuss the results obtained from this formalism.

III. RESULTS AND DISCUSSION

For the results that follow, we have used $M=160\,000$, although we checked that our results did not change (within the error bars) for larger pools of triplets. For all three hierarchical lattices considered, the first moments presented small fluctuations around their initial values [i.e., $\langle K_{ij} \rangle = 0$ and $\langle H_i \rangle$ (either zero or not)] under successive renormalizations. Therefore, our criteria for the identification of the attractors, and their associated phases, were based on the widths σ_K , σ_H , and their ratio r , which showed that the behavior of σ_K always prevailed over the one of σ_H .

We have found typically two distinct behaviors for these quantities, under successive RG transformations, which we associated with two distinct phases as described below. (i) Paramagnetic (P) phase: this occurs for sufficiently large temperatures and/or fields, where $\sigma_K \rightarrow 0$ and $\sigma_H \rightarrow 0$, with $r \rightarrow 0$. (ii) SG phase: this phase appears for low temperatures and fields, being characterized by $\sigma_K \rightarrow \infty$ and $r \rightarrow \infty$. In most of the cases, we have found throughout this phase an increase on σ_H as well, but still keeping $r \rightarrow \infty$; however, in some situations (essentially for symmetric field distributions), we have found that $\sigma_K \rightarrow \infty$ and $\sigma_H \rightarrow 0$. The critical frontier separating these two phases was considered as the one where the parameter r changes very slowly. Typical behaviors of the ratio r , under successive RG transformations, are illustrated in Fig. 2 for an Ising SG on the hierarchical

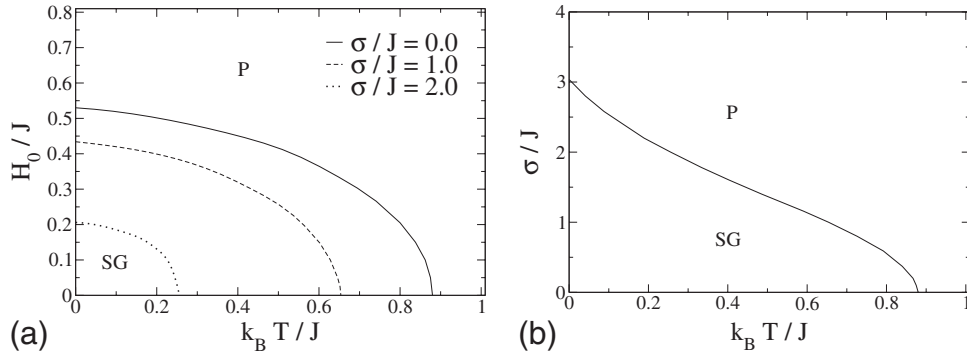


FIG. 3. Phase diagrams for an Ising SG on the hierarchical lattice defined by the unit cell of Fig. 1(a) in the presence of an initial random magnetic field following a Gaussian probability distribution. (a) Plane H_0 vs temperature for different values of σ . (b) Plane σ vs temperature for $H_0=0$. **P** and **SG** denote the paramagnetic and spin-glass phases, respectively.

lattice defined by the unit cell of Fig. 1(a) in the presence of an initial uniform field H_0 . In Fig. 2(a) we present this quantity for different values of H_0/J at zero temperature, whereas in Fig. 2(b), we have fixed the initial field [$(H_0/J)=0.3$] and have varied the temperature; in both figures one sees that the ratio of widths r may present qualitatively distinct behaviors, depending on the initial parameters considered, signaling different attractors of the renormalization.

In Fig. 3 we exhibit phase diagrams obtained from the present RG approach for the Ising SG defined by Eqs. (1), (2), and (5) on the diamond hierarchical lattice of Fig. 1(a). In Fig. 3(a) we present phase diagrams in the plane H_0 versus temperature for different choices of σ ; one notices that for increasing values of σ , the SG phase decreases; a similar effect has been observed in mean-field theory, where this phase is delimited by an AT line, associated with RSB [34]. It is important to stress that the case $\sigma=0$ in Fig. 3(a) corresponds, within the RG procedure, to an initial uniform field; therefore, the uniform and Gaussian random fields produce a qualitatively similar critical frontier. In Fig. 3(b) we show the phase diagram in the plane σ versus temperature, for the case of a symmetric Gaussian distribution for the fields ($H_0=0$), which displays also a SG phase for low temperatures.

In Fig. 4 we exhibit the phase diagram for the present Ising SG model under the bimodal random field defined by Eq. (4). One notices that the critical frontier of Fig. 4 presents a change of concavity for low temperatures and so it is qualitatively different from those of a uniform field [case $\sigma=0$ in Fig. 3(a)] and Gaussian random field [cases $\sigma>0$ in Fig. 3(a)]. Curiously, this critical frontier is very similar to the one of a symmetric Gaussian distribution shown in Fig. 3(b). Analogous to the previous cases, shown in Fig. 3 (uniform and Gaussian random fields), the most important as-

pect, i.e., the existence of the SG attractor, associated with a SG phase at low temperatures applies for the bimodal random field as well.

We have also investigated the present Ising SG model on the hierarchical lattices of Figs. 1(b) and 1(c); although the results are quantitatively different, the qualitative behaviors of the phase diagrams are the same as those shown above for the diamond hierarchical lattice. In Tables I and II we compare critical parameters, associated with the phase diagrams, for the three hierarchical lattices investigated. In Table I we present the values of the critical temperatures for $H_0=0$, in the case of the uniform and bimodal distributions for the fields, whereas for the Gaussian distribution, the results refer to the particular width $(\sigma/J)=1$. In Table II we present values of critical fields, at zero temperature; for a Gaussian distribution, our zero-temperature results correspond to the cases $(\sigma/J)=1$ or $H_0=0$ (cf., e.g., Fig. 3). From these tables one notices that the critical parameters for the hierarchical lattices defined by the cells in Figs. 1(a) and 1(b) are always below and above, respectively, the ones of the hierarchical lattice of Fig. 1(c). This confirms the current belief that these lattices yield lower and upper limits for phase-diagram critical parameters [31]; in addition to that, it suggests that the Wheatstone-Bridge lattice of Fig. 1(c) may lead to good approximations in the study of three-dimensional SG systems. In fact, the corresponding critical-temperature estimate for $H_0=0$ (uniform and bimodal cases) shown in Table I, $(k_B T_c/J)=0.980(1)$, is in good agreement with the recent estimate from Monte Carlo simulations on a cubic lattice, $(k_B T_c/J)=0.951(9)$ [12], leading to a relative discrepancy of 2%, taking into account the error bars.

The results above are reinforced by a zero-temperature analysis of the evolution of the widths associated with the

TABLE I. The critical temperatures for $H_0=0$, with the fields following Eqs. (3)–(5), for the hierarchical lattices defined by the cells of Fig. 1. In the case of the Gaussian distribution for the fields, we have chosen $(\sigma/J)=1$. Error bars refer to the usual approach to criticality characteristic of the RG technique.

Hierarchical lattice	$k_B T_c/J$ Uniform and Bimodal	$k_B T_c/J$ Gaussian [$(\sigma/J)=1$]
Cell 1(a)	0.880(1)	0.661(1)
Cell 1(b)	1.761(1)	1.750(1)
Cell 1(c)	0.980(1)	0.891(1)

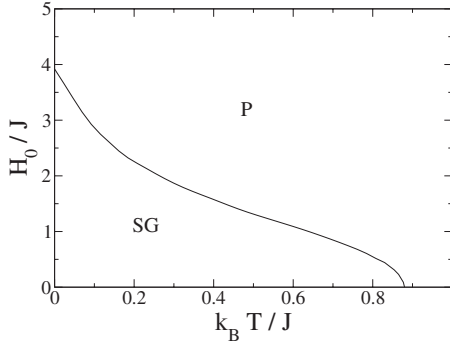


FIG. 4. Phase diagram for an Ising SG on the hierarchical lattice defined by the unit cell of Fig. 1(a) in the presence of an initial random magnetic field following a symmetric bimodal probability distribution.

couplings (σ_J) and fields (σ_H) with respect to the RG steps n ,

$$\sigma_J \sim b^{ny}; \quad \sigma_H \sim b^{nu}, \quad (16)$$

which are characterized by the exponents y (usually known as the stiffness exponent) and u ; the scaling factor is $b=2$ for all three cells of Fig. 1. In Fig. 5 we illustrate the power-law behaviors of Eq. (16) for the case of an initial uniform field H_0 on a hierarchical lattice defined by the unit cell of Fig. 1(a). The values of H_0 chosen in Fig. 5 correspond to zero-temperature points in the spin-glass phase of the case $\sigma=0$ in Fig. 3(a). The scaling range (in the RG steps n) starts for small n (typically around $n=5$) for $0 \leq H_0 \leq H_{0c}/2$, but for larger values of H_0 (essentially as one approaches the critical value H_{0c}) the scaling forms of Eq. (16) are only satisfied for higher ranges of the iteration steps n . We have noticed that, in all cases, the exponents y and u are weakly dependent on the initial value H_0 (as can be seen on the examples shown in Fig. 5); as a consequence of this, we have assumed universality with respect to H_0 for each of these exponents. Our estimates, for the case of an initial uniform field H_0 , are presented in Table III for each of the hierarchical lattices of Figs. 1; the error bars take into account slight variations in these exponents throughout the interval $0 \leq H_0 \leq H_{0c}$. The fact that $y > u$ supports the existence of a low-temperature SG phase based on the criterion described above for the quantity r of Eq. (15).

At this point, it is important to stress that for the families of hierarchical lattices associated with the cells in Figs. 1(a) and 1(b), for which the fractal dimension may be changed easily by varying the number of parallel paths, we have also

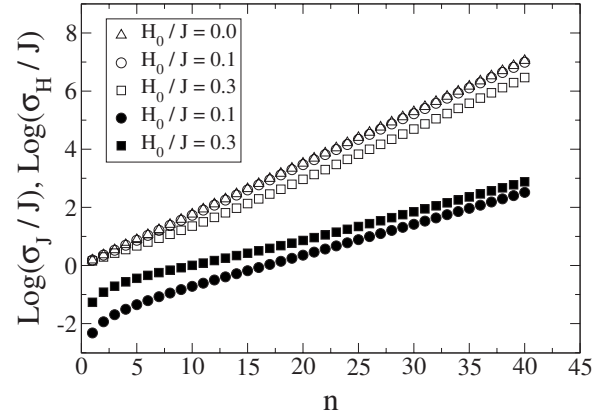


FIG. 5. Evolution of the widths associated with the couplings (σ_J) (empty symbols) and fields (σ_H) (black symbols) with the RG steps n for typical values of an initial uniform field H_0 . In the first case we exhibit also the case $H_0=0$. Base- e logarithms were used.

investigated lattices with fractal dimensions $D < 3$ (more specifically, those characterized by three parallel paths, for which $D \approx 2.585$). In these cases, we did not find any evidence of a SG attractor, suggesting that for these lattices one has a lower critical dimension, $2.585 < D_l < 3$. Taking into account the above-mentioned properties of these lattices, concerning lower and upper limits for the critical temperatures, one may expect that these bounds for the lower critical dimension, associated with a SG phase in the presence of an external magnetic field, should apply to other lattices as well.

To conclude, we have investigated a nearest-neighbor-interaction Ising spin-glass model, in the presence of an external magnetic field, on three different hierarchical lattices that approach the cubic lattice. In the beginning of the renormalization-group procedure, the magnetic field was considered as uniform, or randomly distributed, following either a bimodal or a Gaussian probability distribution. In all cases considered, a spin-glass attractor was found, in the plane magnetic field versus temperature, which was associated with a low-temperature spin-glass phase. In the particular cases of hierarchical lattices for which the fractal dimension may be changed easily by varying the number of parallel paths, we have verified that the lower critical dimension, associated with a finite-temperature spin-glass phase, lies in the interval $2.585 < D_l < 3$. The present results show that, in what concerns the hierarchical lattices studied, *there is a spin-glass phase in the presence of an external magnetic field*, contrary to the claim of recent numerical simulations on the cubic lattice [11,13]. Since the above results concern

TABLE II. Zero-temperature critical values of the fields following Eqs. (3)–(5) for the hierarchical lattices defined by the cells of Fig. 1. In the case of the Gaussian distribution for the fields, we have chosen either $(\sigma/J)=1$ or $H_0=0$. Error bars refer to the usual approach to criticality characteristic of the RG technique.

Hierarchical lattice	Uniform H_{0c}/J	Bimodal H_{0c}/J	Gaussian [$(\sigma/J)=1$]	
			H_{0c}/J	Gaussian ($H_0=0$) σ_c/J
Cell 1(a)	0.530(1)	3.919(1)	0.433(1)	3.036(1)
Cell 1(b)	1.414(2)	21.45(2)	1.418(1)	20.25(2)
Cell 1(c)	0.590(2)	5.907(2)	0.566(2)	5.884(2)

TABLE III. The zero-temperature exponents γ and u [defined in Eq. (16)] for an initial uniform field H_0 in the range $0 \leq H_0 \leq H_{0c}$, where H_{0c} is given in Table II for each of the hierarchical lattices defined by the cells of Fig. 1.

Hierarchical lattice	Exponent γ	Exponent u
Cell 1(a)	0.245(8)	0.140(8)
Cell 1(b)	0.254(2)	0.002(1)
Cell 1(c)	0.223(2)	0.007(3)

the existence of a spin-glass attractor, under renormalization-group transformations, the question of replica-symmetry breaking throughout this phase, which would characterize the critical lines presented herein as Almeida-Thouless lines, represents a point that deserves further investigations. Taking

into account that hierarchical lattices have been a useful tool for studying spin-glass systems, the present results motivate the investigation of replica-symmetry-breaking properties for spin glasses on hierarchical lattices in the presence of external magnetic fields. It is possible that the picture found previously on the $D=3$ Migdal-Kadanoff hierarchical lattice, without a magnetic field [18,21,22,24], exhibiting replica-symmetry-breaking characteristics only close to the critical temperature, may change under the presence of an external magnetic field.

ACKNOWLEDGMENTS

We thank Professor E. M. F. Curado for fruitful conversations. The partial financial supports from CNPq and Pronex/MCT/FAPERJ (Brazilian agencies) are acknowledged.

-
- [1] V. Dotsenko, *Introduction to the Replica Theory of Disordered Statistical Systems* (Cambridge University Press, Cambridge, UK, 2001).
- [2] H. Nishimori, *Statistical Physics of Spin Glasses and Information Processing* (Oxford University Press, Oxford, 2001).
- [3] *Spin Glasses and Random Fields*, edited by A. P. Young (World Scientific, Singapore, 1998).
- [4] K. H. Fischer and J. A. Hertz, *Spin Glasses* (Cambridge University Press, Cambridge, UK, 1991).
- [5] B. W. Southern and A. P. Young, *J. Phys. C* **10**, 2179 (1977).
- [6] R. N. Bhatt and A. P. Young, *Phys. Rev. Lett.* **54**, 924 (1985).
- [7] A. T. Ogielski and I. Morgenstern, *Phys. Rev. Lett.* **54**, 928 (1985).
- [8] A. J. Bray and M. A. Moore, in *Heidelberg Colloquium on Glassy Dynamics*, Lecture Notes in Physics 275, edited by J. L. van Hemmen and I. Morgenstern (Springer-Verlag, Berlin, 1987).
- [9] R. N. Bhatt and A. P. Young, *Phys. Rev. B* **37**, 5606 (1988).
- [10] E. Marinari, G. Parisi, and J. J. Ruiz-Lorenzo, in *Spin Glasses and Random Fields*, edited by A. P. Young (World Scientific, Singapore, 1998).
- [11] A. P. Young and H. G. Katzgraber, *Phys. Rev. Lett.* **93**, 207203 (2004).
- [12] H. G. Katzgraber, M. Körner, and A. P. Young, *Phys. Rev. B* **73**, 224432 (2006).
- [13] T. Jörg, H. G. Katzgraber, and F. Krzakala, *Phys. Rev. Lett.* **100**, 197202 (2008).
- [14] J. R. Banavar and A. J. Bray, *Phys. Rev. B* **35**, 8888 (1987).
- [15] J. R. Banavar and A. J. Bray, *Phys. Rev. B* **38**, 2564 (1988).
- [16] M. Nifle and H. J. Hilhorst, *Phys. Rev. Lett.* **68**, 2992 (1992).
- [17] F. D. Nobre, *Phys. Lett. A* **250**, 163 (1998).
- [18] M. A. Moore, H. Bokil, and B. Drossel, *Phys. Rev. Lett.* **81**, 4252 (1998).
- [19] E. Nogueira, Jr., S. Coutinho, F. D. Nobre, and E. M. F. Curado, *Physica A* **271**, 125 (1999).
- [20] E. M. F. Curado, F. D. Nobre, and S. Coutinho, *Phys. Rev. E* **60**, 3761 (1999).
- [21] E. Marinari, G. Parisi, J. J. Ruiz-Lorenzo, and F. Zuliani, *Phys. Rev. Lett.* **82**, 5176 (1999).
- [22] H. Bokil, A. J. Bray, B. Drossel, and M. A. Moore, *Phys. Rev. Lett.* **82**, 5177 (1999).
- [23] F. D. Nobre, *Physica A* **280**, 456 (2000).
- [24] B. Drossel, H. Bokil, M. A. Moore, and A. J. Bray, *Eur. Phys. J. B* **13**, 369 (2000).
- [25] F. D. Nobre, *Phys. Rev. E* **64**, 046108 (2001).
- [26] F. D. Nobre, *Physica A* **319**, 362 (2003).
- [27] G. Parisi, *Phys. Rev. Lett.* **43**, 1754 (1979); **50**, 1946 (1983).
- [28] J. R. L. de Almeida and D. J. Thouless, *J. Phys. A* **11**, 983 (1978).
- [29] D. Badoni, J. C. Ciria, G. Parisi, F. Ritort, J. Pech, and J. J. Ruiz-Lorenzo, *Europhys. Lett.* **21**, 495 (1993).
- [30] F. Krzakala, J. Houdayer, E. Marinari, O. C. Martin, and G. Parisi, *Phys. Rev. Lett.* **87**, 197204 (2001).
- [31] J. R. Melrose, *J. Phys. A* **16**, 1041 (1983).
- [32] A. Rosas and S. Coutinho, *Physica A* **335**, 115 (2004).
- [33] M. S. Cao and J. Machta, *Phys. Rev. B* **48**, 3177 (1993).
- [34] R. F. Soares, F. D. Nobre, and J. R. L. de Almeida, *Phys. Rev. B* **50**, 6151 (1994).